

Full Length Article

Defects studies of nickel aluminum bronze subjected to cavitation

K. Siemek^{a,b,*}, M.K. Eseev^{a,c}, P. Horodek^b, A.G. Kobets^{a,d}, I.V. Kuziv^c^a Joint Institute for Nuclear Research, Joliot-Curie 6, 141980 Dubna, Moscow Region, Russia^b Institute of Nuclear Physics Polish Academy of Sciences, PL-31342 Krakow, Poland^c Northern Arctic Federal University, 163002 Severnaya Dvina Emb. 17, Arkhangelsk, Russian Federation^d Institute of Electrophysics and Radiation Technologies, NAS of Ukraine, Chernyshevsky St. 28, 61002 Kharkov, Ukraine

ARTICLE INFO

Keywords:

Cavitation

Positron annihilation

Defects

Cavitation erosion

ABSTRACT

A defects evolution below the surface in nickel aluminum bronze CuAl9Ni4Fe4 subjected to cavitation under mild conditions with times up to 8 h was studied using positron annihilation spectroscopy, mass loss measurements, and scanning electron and atomic force microscopies. The obtained results indicate two different stages of cavitation erosion. At the beginning of cavitation up to 6 h in incubation period a removing of residual roughness and surface oxides was noted. Then, in the maximal erosion rate region, big vacancy clusters were recognized and their concentration drastically increases around 100 times in comparison with the incubation period.

1. Introduction

Cavitation is a dynamic process of the formation and implosion of cavities in fluids caused by sudden pressure drops. This phenomenon is mostly regarded to be destructive and contributes to wear and failure of elements in fluid-flow machines. Cavitation erodes materials by the following mechanisms: generation of shock waves due to symmetric bubble implosion which can result in material fatigue and plastic deformation, and formation of microjets resulting from the asymmetrical collapse of the vapor bubbles near the material surfaces [1,2]. Due to unique type of loading, the cavitation erosion resistance of a material depends on many factors such as materials properties and machining methods, the fluid properties, and the flow field characteristic [2,3,4,5]. On the other hand, cavitation can be used as a subsurface modification method, which improves its fatigue properties and hardness [6,7]. This application of cavitation is mostly related to ultrasonic cavitation peening. In both processes, a characteristic defect profile beneath the surface is established.

Recently, the wear resistance and degree of damage of eroded materials is mostly determined based on parameters such as cumulative mass and volume loss or a mean depth of cavitation erosion [2,3,8]. The typical cavitation erosion-time curve can be subdivided into three areas: incubation period (IP), acceleration or maximal erosion rate region (MER), and attenuation stage (AS) [1,3,6]. In the first one plastic deformations occur in the subsurface region but no measurable mass loss is observed. Then, the erosion rate drastically increases in MER and finally

slows down in AS because rough strongly fractured surface acts as a kind of protective cushion. Erosion pits are obvious characteristics on the surface and their development can describe the cavitation erosion process. However, the surface and subsurface characteristics in different erosion stages cannot be found from the loss curve. Alternative methods including the evolution of surface roughness [3,4,8] quantify erosion damage have only been scarcely reported.

In the last decades, a positron annihilation spectroscopy has been attracting increasing attention in defects subsurface studies. In comparison to other typical methods used like SEM or TEM it gives insight on damages below the sample surface and makes it possible to observe defects evolution during cavitation. This method allows studying concentrations and types of open volume voids in materials, i.e. vacancies and their clusters, dislocations, pores. The successful application of this method was proven in numerous studies for various processes, such as friction [9], ion implantation [10], sandblasting [11]. It was also used to determine defects in mild steel subjected to cavitation during times up to 40 min [12]. The results of this work show that vacancy concentration growth and its agglomeration is observed with increasing time of cavitation. However, the studied cavitation period responds only to the incubation of damages and does not allow to observe defects evolution when erosion starts.

In current studies, we investigate cavitation damages after a different period of treatment time up to 8 h for a nickel aluminum pressureless tinless bronze commonly used in marine propellers with nominal composition CuAl9Ni4Fe4. The major aim of studies concentrates on the

* Corresponding author.

E-mail address: krzysztof.siemek@ifj.edu.pl (K. Siemek).

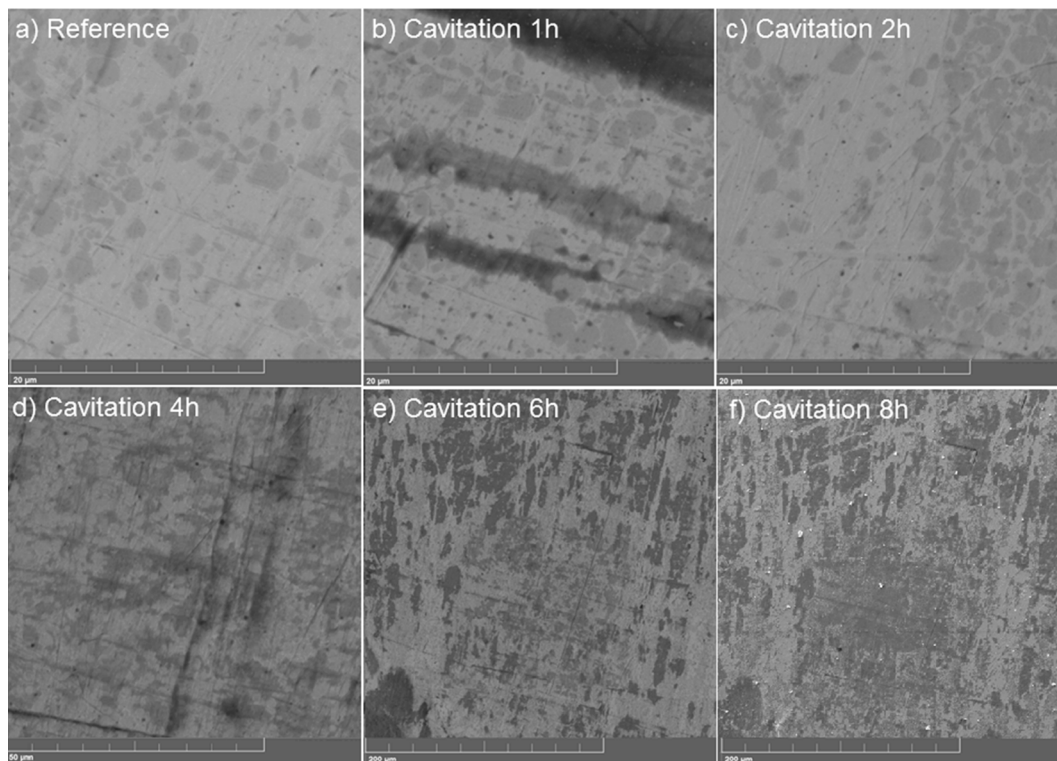


Fig. 1. SEM images of the surface of CuAl9Ni4Fe4 alloy subjected to cavitation with different period time.

determination of damages on surface and also below it for different erosion stages. The evolution of the surface topography was studied with a scanning electron microscope (SEM) and atomic force microscope (AFM). The subsurface defects and its depth profile was investigated using positron lifetime and Doppler broadening of annihilation line spectroscopies.

2. Experiment

For the measurements commercial nickel aluminum tinless bronze with nominal composition CuAl9Ni4Fe4 was selected. Each of 13 specimen in form of plates with surface area $1 \text{ cm} \times 1 \text{ cm}$ and thickness 1 mm was polished to reach the surface roughness lower than $0.1 \text{ }\mu\text{m}$. Then samples were annealed at $600 \text{ }^\circ\text{C}$ for 3 h to remove the defects created during sample preparation. The annealing was performed in vacuum 10^{-5} Torr to avoid expanding of oxides below the surface. The state of all annealed samples were checked before cavitation using positron lifetime spectroscopy and did not show presence of any defects. Pairs of samples were subjected to cavitation with different time periods in exactly the same conditions and two of them were kept as reference ones. In the positron lifetime measurements two samples were used, while for other measurements only one of this pair of samples without any changes of its surface. One additional sample was predicted to cumulative mass and cumulative mass rate curve measurements. Cavitation was performed using the ultrasonic generator MEF93.1 (MEFLFIZ-Ultrazvuk OOO) with frequency $23 \pm 1 \text{ kHz}$. Horn diameter was 12 mm and the working distance between the horn tip and the exposed specimen surface was set to 8 mm. The chosen distance corresponds, according to our estimates, to the energy effect per unit area of the propeller and it is much lower than the standard ASTM G32 predicted for very fast cavitation tests. The specimen was placed 30 mm under the free liquid level. The treatment temperature was around $25 \text{ }^\circ\text{C}$ and controlled using a thermocouple and a pellet control element that regulates the temperature in the sample bath. During the treatment temperature changes in range $24\text{--}28 \text{ }^\circ\text{C}$ was noted.

3. Methods

Samples were investigated by atomic force microscopy in semi-contact mode and scanning electron microscopy in secondary electron mode. The surface characterization was performed using Scanning Electron Microscope Tescan Vega3 SBH and Atomic Force Microscope AFM/STM SOLVER Nano (NT-MTD). The roughness characteristics $R_q = \sqrt{\frac{1}{n} \sum_{i=1}^n y_i^2}$, (where y is the deviations in the high direction) was calculated using Image Analysis 3.5 and averaged over five random profiles of sampling length $100 \text{ }\mu\text{m}$ at each test time near the central region of the area subjected to cavitation.

The positron lifetime (LT) measurements were conducted using digital spectrometer APU-8702RU and the BaF₂ scintillators with the timing resolution equaled about 200 ps. The typical sandwich geometry was used, where the positron source was located between to identically prepared samples. The source was built from ²²Na isotope enclosed into thin two $5 \text{ }\mu\text{m}$ thick titanium foils. Around 15% of all positrons annihilate in source with lifetimes 242 ps (97%) and 972 ps (3%). This contribution and background were taken into account in the deconvolution procedure. The analysis of spectra was conducted using LT 10.2 program. All spectra include at least 2×10^6 counts. Around 63% of all positrons annihilate up to $23 \text{ }\mu\text{m}$, which corresponds to the mean positron implantation depth and approximated studied area.

The Doppler broadening of annihilation line measurements was performed using the ORTEC HPGe detector model GEM25P4-70 with energetic resolution FWHM 1.2 keV at 0.511 MeV line. The similar source based on ²²Na isotope like in positron lifetime measurements was used to determine the damaged zone range. The experiment was performed using a sequential etching procedure. It means that after each etching step, in which around $5 \text{ }\mu\text{m}$ of subsurface was removed, an S parameter beneath the surface was evaluated. S parameter is defined as ratio of surface area under the central part of the 511 keV line to total surface area under this line. Its changes are linked with the momentum of annihilated electrons. It increases with defects concentration but in a non-linear way and also depends on the type of defect.

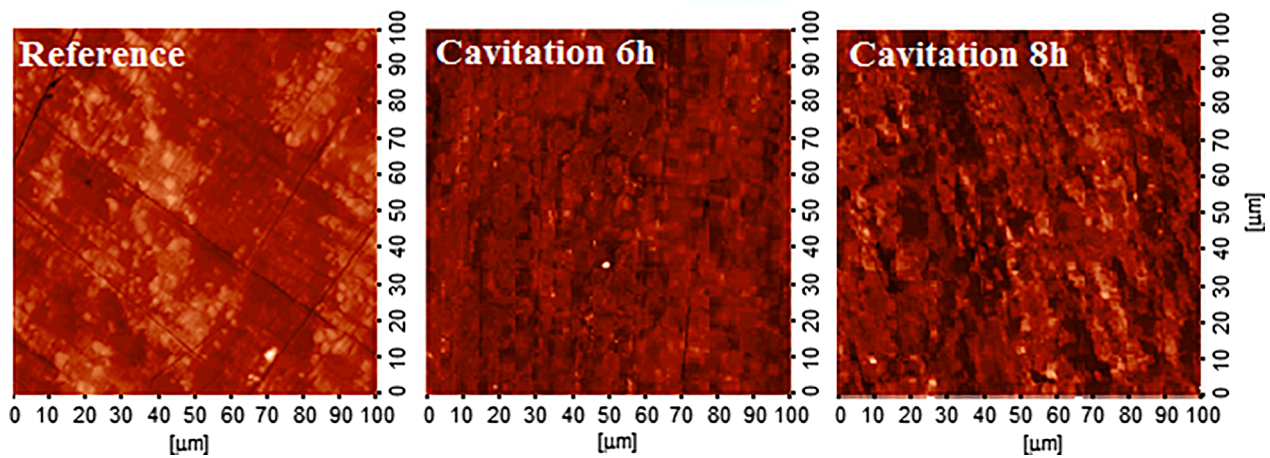


Fig. 2. AFM images of the surface of CuAl9Ni4Fe4 alloy subjected to cavitation with different period time.

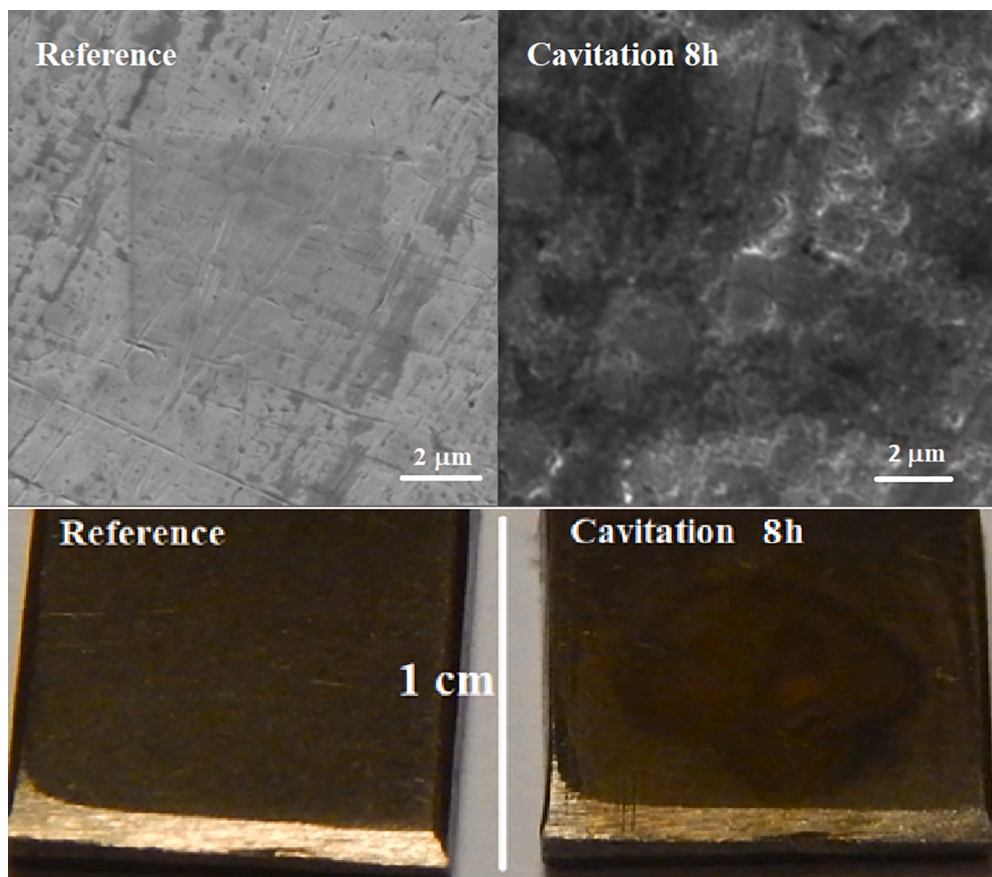


Fig. 3. Photograph and SEM images (with higher magnification) of CuAl9Ni4Fe4 alloy before and after 8 h cavitation test.

The last used method is based on slow monoenergetic beam with positrons energies ranging up to 35 keV working at JINR in Dubna, Russia. Moderation of positron energies emitted from ^{22}Na isotope gives the ability to study precisely defects in the most interesting near surface region up to 1.1 μm , where the observed defects can be connected with SEM and AFM microscopies observations. These studies were conducted using the Doppler broadening of the annihilation line method.

4. Results and discussion

The observation of surface topography and cumulative mass loss can

describe the cavitation erosion process. The SEM and AFM images of samples after different cavitation periods are shown in Figs. 1, 2, respectively. The size of eroded area after 8 h treatment is shown in a photograph, Fig. 3. In Figs. 1 and 2, small hills in reference samples can be observed. These surface irregularities are slowly removed up to 6 h treatment and are also related to changes of roughness R_q , presented in Fig. 4a. R_q firstly rise with cavitation time for the sample treated for 1 h and then slowly decreases up to 6 h. Cumulative mass losses present in Fig. 4b show that in this stage only small mass losses are observed which is characteristic for the incubation period. Beginning from treatment time 8 h R_q drastically increases and a strongly fractured surface with

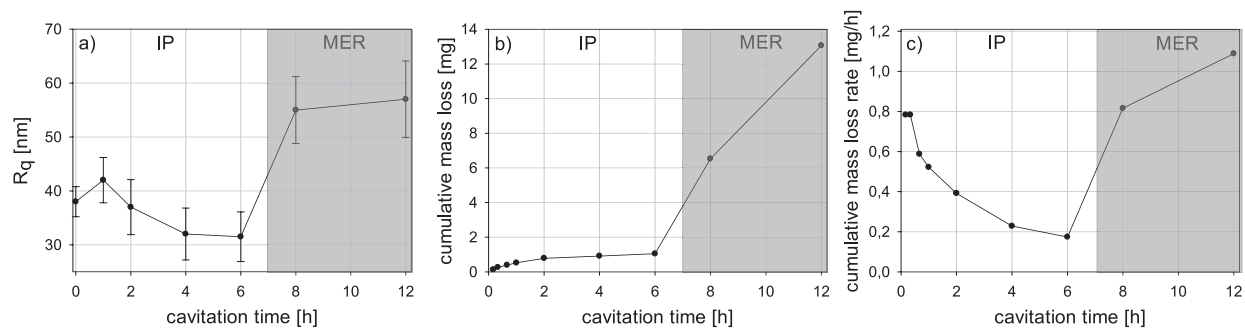


Fig. 4. Roughness R_q (a), cumulative mass loss (b) and cumulative mass loss rate (c) in a function of cavitation time. On plots, two characteristics erosion stage: incubation period (IP), maximal erosion rate region (MER) were marked.

Table 1

Positron lifetime for CuAl9Ni4Fe4 alloy subjected to cavitation at different times. τ_1 and τ_2 represent positron lifetime components and I_1 and I_2 its intensities, respectively. τ_{av} is a mean positron lifetime.

Sample description	τ_1 [ps]	I_2 [%]	τ_2 [ps]	τ_{av} [ps]
reference	130 (1)	–	–	130 (1)
cavitation 1 h	142 (1)	18 (1)	281 (1)	168 (1)
cavitation 2 h	98 (1)	61 (1)	180 (1)	149 (1)
cavitation 4 h	117 (1)	32 (1)	197 (1)	143 (1)
cavitation 6 h	110 (1)	43 (1)	165 (1)	134 (1)
cavitation 8 h	126 (1)	10 (1)	246 (1)	138 (1)

lots of pits can be observed both in SEM and AFM images. Also sharp increase of cumulative mass losses and mass loss rate confirm beginning of new cavitation erosion stage MER, see Fig. 4b and 4c. Only two stages can be distinguished in cumulative mass loss plot for studied cavitation time treatment which are IP, MER. They have been marked in Fig. 4. Previously reported period times of IP and MER for brass (30 wt% Zn) by Chiu et al. [3] indicate that it finishes over 40 min and 245 min. In current studies IP is much longer and takes 420 min due to mild condition of cavitation process caused by large distance between samples and ultrasonic generator horn tip. In many studies [3,4,8], the surface roughness only increases with cavitation time. Here, firstly the lowering of initial reference sample roughness in IP period was found (Fig. 4), without traces of mean depth cavitation erosion. This should be described as removing of surface oxides which has different properties than bronze interior.

Positron lifetime measurement was performed to determine the defect type after cavitation. According to the available literature, the positron lifetime studies on alloy CuAl9Ni4Fe4 or similar copper bronze were not reported, therefore, the obtained results will be confronted with pure Cu. The positron lifetime for well-annealed samples was 130 ps and correspond well with $\tau = 122$ ps of defect-free copper reported by Hinode [13]. A small difference in values should be assigned to the presence of alloying additions. Two lifetime components were resolved from the lifetime spectra in samples subjected to cavitation. They correspond to positron annihilation in various types of defects and from the free state (the annihilation from the Bloch delocalized states). Its values are gathered in Table 1. CuAl9Ni4Fe4 samples treated by 1 h time are the most deformed one. For these samples dislocations (with corresponding lifetime component $\tau_1 = 142$ ps) and clusters consisting of 7 vacancies (for which $\tau_2 = 281$ ps) were found, see Table 1. The size of the vacancies clusters was estimated using Zhou et al. [14] calculations performed for pure copper. No annihilation free component was noted for 1 h cavitation period which indicates that all positrons annihilate in defects and no positrons reach undamaged part of the sample. However, this component appears for other samples and corresponds to τ_1 values smaller than 130 ps. The magnitude of the reduction of free positrons τ_1 depends on the number of positrons which annihilate inside defect and it is proportional to the intensity I_2 [15]. For all samples treated at least 2

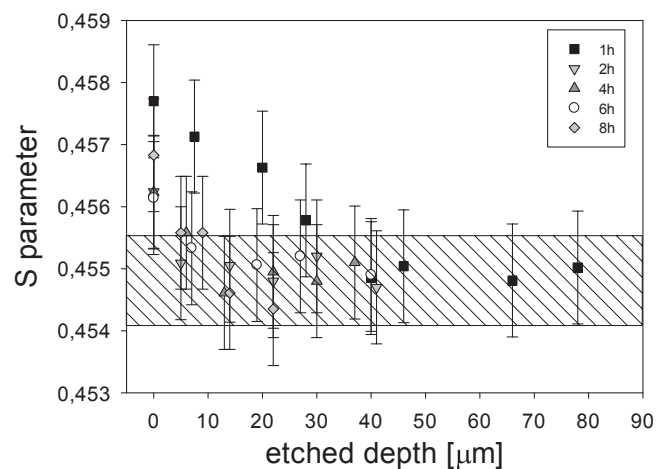


Fig. 5. S parameter dependency in the function of etched depth for CuAl9Ni4Fe4 alloy after different cavitation period for conventional Doppler broadening annihilation method employing ^{22}Na isotope source.

h, the positrons trapped in defects are therefore described only by τ_2 , and its intensity I_2 correlates with defects concentration. A higher value of τ_2 stands for bigger vacancy clusters size. It changes during cavitation and correlates with cumulative mass loss rate in Fig. 4c. Firstly, the decrease of its size is observed to divacancies in samples treated by 2 h and 4 h and then after 6 h only monovacancies can be seen. After 8 h, a MER stage starts and a bigger vacancies agglomerates cluster consists of 5 vacancies appear again. Also mean positron lifetime $\bar{\tau} = \tau_1 I_1 + \tau_2 I_2$ can be used to monitoring the cavitation erosion. Its behavior is similar to the τ_2 component, i.e. the highest $\bar{\tau}$ value was noted for the shortest cavitation period time and then it decreases with treatment time up to 6 h. Previously reported studies of damages caused by the cavitation process by Zhao et al. [12] in mild steel indicate that the mean positron lifetime increases with cavitation time up to 40 min and is linked with the formation of vacancy clusters. In the work [12] only incubation stage was studied, and probably no surface layer was removed. Continuous plastic deformation during cavitation causes an increment of the number of defects in the subsurface and their clustering in the IP. It also affects mechanical properties such as hardness [6]. After exceeding the IP, defect types and their depth distribution in the material due to erosion can change significantly.

The Doppler broadening measurement was used to study defect profiles beneath the surface. The measurements using conventional ^{22}Na source were done repeatedly with etching in a solution of nitric and hydrofluoric acid in molar ratio 1:3. The S parameter as a function of etched depth is shown in Fig. 5. The hatched area corresponds to the sample without defects. In all cases S parameter decreases with the depth, and finally reaches the value of the well-annealed sample. In

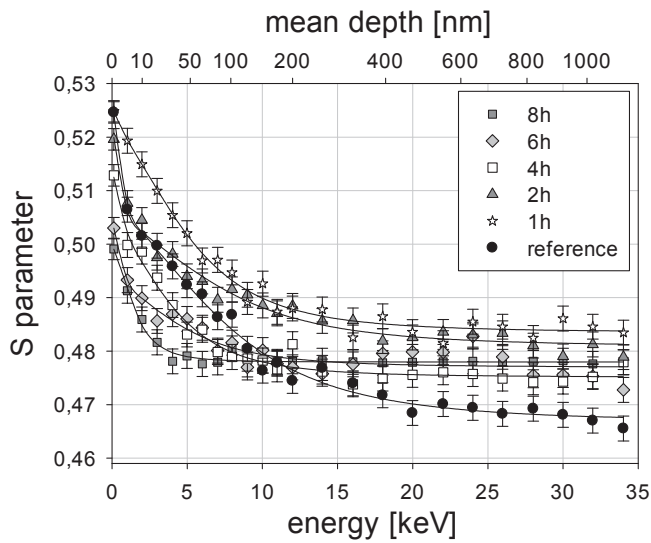


Fig. 6. S parameter dependency in the function of positron energy (bottom axis) and mean implantation depth (upper axis) for CuAl9Ni4Fe4 alloy after different cavitation period performed using variable energy positron beam. The solid lines presents the best fits obtained using VEPFIT program.

sample after 1 h cavitation the reference state is reached after etching around 30 μm , and for other samples after removing around 5 μm of the subsurface zone. This indicates a shallow depth of defects occurrence for samples treated 2 h and longer periods and justifies the use of positron beam measurements.

Before etching samples were also investigated using variable energy slow positrons beam. In Fig. 6 the results of these measurements are shown. The mean implantation depth presented in upper axis was calculated according to the equation:

$$\bar{z} = \frac{A}{\rho} E^n, \quad (1)$$

where A and n are the Makhov function parameters and $\rho = 8.96 \text{ g/cm}^3$ is the density of a material. The values $n = 1.647$ and $A = 2.84 \mu\text{gcm}^2\text{keV}^n$ reported for copper was used in evaluation [16]. The S parameter decreases with positron energies and finally saturates at depths over 500 nm. The rate of drop increases with defects concentration and is related to positron diffusion length L_+ :

$$C = \frac{(L_{\text{bulk}}/L_+)^2 - 1}{\tau_{\text{bulk}}\mu}, \quad (2)$$

where $\tau_{\text{bulk}} = 130 \text{ ps}$, μ is the trapping coefficient for a single vacancy assumed in present calculations as 10^{15} s^{-1} , and $L_{\text{bulk}} = 112 \text{ nm}$. The analysis of results was performed using the VEPFIT program [17], which solves the full positron implantation-diffusion model. A one-layer model was fitted with a specific S parameter value for sample interior S_{Interior} and its surface S_{Surface} . Also, the positron diffusion length was determined. The changes in these parameters are shown in Fig. 7a. The S_{Surface} starts to decrease after two-hour cavitation period. The reduction of this parameter should be regarded as erosion process, which slowly removes the protective oxide layer on the sample surface and changes its chemical composition. The S_{Interior} increases with cavitation time in comparison with a reference sample, which indicates the presence of open volume defects below the surface. Its value is higher for samples treated 1 and 2 h and remains similar for longer times. This may be due to the presence of bigger vacancy clusters, which occurrence was proven using positron lifetime method. The biggest clusters were noted for shortest cavitation time. According to calculations of Luna et al. [18], the S parameter for copper should increase with the size of the clusters. The positron diffusion length decreases after cavitation, which stands for an increased number of defects below the surface. According to Eq. (2), the defect concentrations C_D in samples are equal 21, 10, 52, 25, 1524 ppm for samples treated 1, 2, 4, 6, and 8 h, respectively. These values were plotted in Fig. 7b. It is interesting that although the concentration of defects is the highest for the longest cavitation time, their depth distribution is small and ends below 5 μm , see Fig. 5. Near 100-times difference in defect concentration in comparison with other shorter period indicate a change of stage of material cavitation erosion to MER.

5. Conclusion

During the cavitation process performed for different times up to 8 h in mild conditions in nickel aluminum bronze, a defects evolution below the surface was observed. Two cavitation erosion stages were studied: incubation period (IP) and maximal erosion rate (MER) stage. The obtained results indicated that the size and number of microdefects change in these stages. In the beginning of treatment after 1 h period, the defects occupy the biggest depth of up to 30 μm . They were determined as clusters consisting of 7 vacancies and dislocations. Then up to 6 h the surface is flattered and only divacancies and monovacancies were observed. The area of their occurrence was drastically reduced. In the MER region, the agglomerated vacancies appeared again and was built with 5 vacancies. However, their depth range below the surface has not

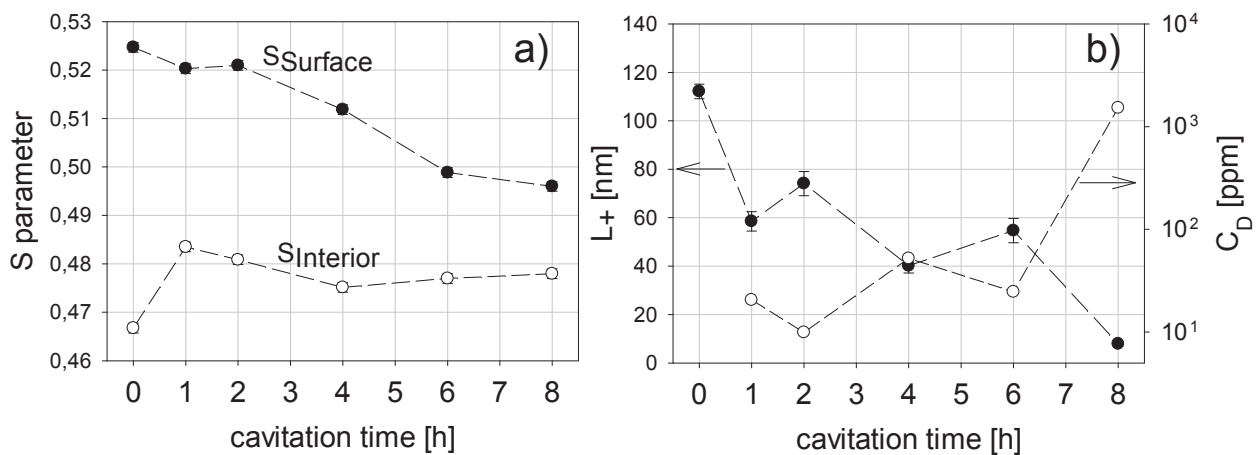


Fig. 7. Adjusted parameters values of S_{Surface} , S_{Interior} (a), and positron diffusion length L_+ (b) obtained using VEPFIT for fitted curves in Fig. 6 for CuAl9Ni4Fe4 bronze subjected to cavitation. In b) evaluated defects concentration C_D was also plotted.

changed drastically. Variable energy slow positrons show that concentrations of these defects in the range up to 1 μm drastically increase around 100 times in comparison with IP stage.

CRedit authorship contribution statement

K. Siemek: Conceptualization, Writing - original draft, Writing - review & editing, Methodology, Formal analysis, Investigation. **M.K. Eseev:** Conceptualization, Funding acquisition. **P. Horodek:** Writing - review & editing. **A.G. Kobets:** Investigation. **I.V. Kuziv:** Investigation.

Declaration of Competing Interest

The authors declare that they have no known competing financial interests or personal relationships that could have appeared to influence the work reported in this paper.

Acknowledgments

The work was partially supported by the RFBR grant No. 17-42-290138 "Dynamics of the development of defects in the structure of metals due to cavitation and corrosion effects in hydrodynamic media".

Contributions

K.Siemek: Conceptualization, Writing - Original Draft, Writing - Review & Editing, Methodology, Formal analysis, Investigation M.K.Eseev: Conceptualization, Funding acquisition P.Horodek: Writing - Review & Editing A.G.Kobets: Investigation, I.V.Kuziv: Investigation.

References:

- [1] B.V. Hubballi, V.B. Sundur, A review on the prediction of cavitation erosion inception in hydraulic control valves, *Int. J. Emerg. Technol. Adv. Eng.* 3 (2013) 110.
- [2] W.M.N. Nour, U. Dulas, J. Schneider, K.-H.Z. Gahr, The effect of surface finish and cavitating liquid on the cavitation of alumina and silicon carbide ceramics, *Ceram. –Silik.* 51 (2007) 30.
- [3] K.Y. Chiu, F.T. Cheng, H.C. Man, Evolution of surface roughness of some metallic materials in cavitation erosion, *Ultrasonics* 43 (2005) 713.
- [4] J.D. Escobar, E. Velásquez, T.F.A. Santos, A.J. Ramirez, D. López, Improvement of cavitation erosion resistance of a duplex stainless steel through friction stir processing (FSP), *Wear* 297 (2013) 998.
- [5] C. Haosheng, L. Yongjian, C. Darong, W. Jiadao, Experimental and numerical investigations on development of cavitation erosion pits on solid surface, *Tribol. Lett.* 26 (2007) 153.
- [6] J. Stýková, M. Müller, J. Hujer, The improvement of the surface hardness of stainless steel and aluminium alloy by ultrasonic cavitation peening, *EPJ Web Conf.* 143 (2017) 02119.
- [7] L. Zhu, Y. Guan, Y. Wang, Z. Xie, J. Lin, Influence of process parameters of ultrasonic shot peening on surface nanocrystallization and hardness of pure titanium, *Int. J. Adv. Manuf. Technol.* 89 (2017) 1451.
- [8] H.X. Hu, Y.G. Zheng, C.P. Qin, Comparison of Inconel 625 and Inconel 600 in resistance to cavitation erosion and jet impingement erosion, *Nucl. Eng. Des.* 240 (2010) 2721.
- [9] J. Dryzek, K. Siemek, Positron annihilation studies of subsurface zone created during friction in pure silver, *Tribol. Trans.* 62 (4) (2019) 658.
- [10] K. Siemek, J. Dryzek, M. Mitura-Nowak, A. Lomygin, M. Schabikowski, Positron annihilation studies of long range effect in Ar, N and C ion-implanted silicon, *Nucl. Instrum. Meth.* 465 (2020) 73.
- [11] P. Horodek, K. Siemek, J. Dryzek, M. Wróbel, Impact of abrasant size on damaged zone of 304 AISI steel characterized by positron annihilation spectroscopy, *Metall. Mater. Trans. A* 50 (2019) 1502–1508.
- [12] M. Zhao, J. Wang, D. Chen, X. Hao, B. Wang, Positron annihilation study of the micro-defects induced by cavitation in mild steel, *Phys. B Condens. Matter.* 403 (2008) 2594.
- [13] K. Hinode, S. Tanigawa, M. Doyama, Positron lifetimes in deformed copper, *J. Phys. Soc. Jpn.* 41 (1976) 2037.
- [14] K. Zhou, T. Zhang, Z. Wang, Positron lifetime calculation for possible defects in nanocrystalline copper, *Phys. Scr.* 90 (2015), 105701.
- [15] R.W. Siegel, Positron annihilation spectroscopy, *Annu. Rev. Mater. Sci.* 10 (1) (1980) 393.
- [16] J. Dryzek, P. Horodek, GEANT4 simulation of slow positron beam implantation profiles, *Nucl. Instrum. Meth. B* 266 (2008) 4000.
- [17] A. van Veen, H. Schut, M. Clement, A. Kruseman, M.R. Ijpm, J.M.M. de Nijs, VEPFIT applied to depth profiling problems, *Appl. Surf. Sci.* 85 (1995) 216.
- [18] C.R. Luna, C. Macchi, A. Juan, A. Somoza, Vacancy clustering in pure metals: some first principle calculations of positron lifetimes and momentum distributions, *J. Phys. Conf. Ser.* 443 (2013), 012019.